DISCRETE AND CONTINUOUS
DYNAMICAL SYSTEMS SERIES B

doi:10.3934/dcdsb.2022017

THE ROLE OF VIGILANCE ON A DISCRETE-TIME PREDATOR-PREY MODEL

Ziyad AlSharawi

Department of Mathematics and Statistics
American University of Sharjah, P. O. Box 26666
Sharjah, UAE

Nikhil Pal*

Department of Mathematics
Visva-Bharati
Santiniketan 731235, India

Joydev Chattopadhyay

Agricultural and Ecological Research Unit
Indian Statistical Institute
203, B. T. Road, Kolkata 700108, India

(Communicated by Shigui Ruan)

Abstract. The change of behaviors of prey in the form of vigilance significantly affects the dynamics of a predator-prey system. In this paper, we consider a discrete-time predator-prey model, where the vigilance of prey acts as a trade-off between the safety and growth rate of the prey. Mathematical properties such as stability, permanence, both flip and Neimark-Sacker bifurcations of the model are investigated. Numerical simulations are carried out to illustrate the analytical findings and to explore the impact of prey vigilance on the dynamics of the system.

1. **Introduction and the mathematical model.** Predation is one of the key forces that drive the evolution of a species [14]. The fear of predation hazard may modify both the behavior and physiology of prey, and in the last three decades this truth has become clear to the ecologists [11]. Recently, several authors studied the role of predator's fear on prey populations both theoretically and experimentally [22, 15, 16, 23, 20]. In behavioral ecology, "How prey species thrive under predation risk?" is one of the most investigated issues. The prey population uses different types of anti-predator responses to reduce predation risk. Many researchers considered the vigilance of prey species as a part of anti-predator behavior [4, 21, 3]. Vigilance is an anti-predator behavior and a survival policy of the prey population for examining the surroundings for predators, which is a common phenomenon in population biology. The vigilance of the prey population can vary with group size, location in a herd, presence of juveniles, etc [4]. Many studies showed that prey

2020 *Mathematics Subject Classification.* 92D25, 39A28, 39A33.

Key words and phrases. Predator-prey model, vigilance, stability, flip bifurcation, Neimark-Sacker bifurcation, chaos control.

The first author is supported by AUS grant FRG19-S-S141.

*Corresponding author: Nikhil Pal.

populations increase their vigilance when predation hazard is high. It is to be noted that vigilance interferes with foraging activity and, as a result, the consumption rate of food by prey decreases with an increase of vigilance. On the other hand, vigilance reduces predation pressure and slows down the energy movement from prey populations to the predator populations. Therefore, it is very important to study how varied vigilance influences a predator-prey system. In literature, a few authors studied the impact of prey vigilance on the dynamics of a system with the help of mathematical modeling. Kimbrell *et al.* [9] studied the influence of vigilance on an intraguild predation model. Recently, Malone *et al.* [12] studied the impact of prey vigilance in a continuous-time Lotka-Volterra predator-prey model in the context of inverted biomass pyramids. To the best of our knowledge, the literature lacks studies that consider vigilance in discrete-time predator-prey models. In the present study, we investigate the role of vigilance of prey on the dynamics of a discrete-time predator-prey system.

To facilitate readers' understanding, we describe each step of our model formulation in detail. Here, first of all it is taken into account that the prey population show logistic growth in the absence of predators and this logistic growth is determined based on three factors, namely: a birth rate, a natural death rate and a depletion in the growth rate due to intra-specific competition. So, the actual growth of the prey population in discrete-time setup is presented by the following difference equation [13]:

$$\left\{ \begin{array}{lcl} x_{n+1} & = & x_n exp\big(r-d-ax_n\big), \end{array} \right. \tag{1.1}$$

where x_n denotes the density of prey population at the n-th generation, r is the birth rate of prey, d represents the prey's natural death rate, and the parameter a is related to the intra-species competition.

Next, we consider the interaction among prey and predator species, which follows Holling type-I response function and is described by the following pair of difference equations:

$$\left\{ \begin{array}{lcl} x_{n+1} & = & x_n exp\bigg(r-d-ax_n-py_n\bigg), \\ y_{n+1} & = & y_n exp\bigg(\mu p x_n-m\bigg), \end{array} \right. \tag{1.2}$$

where y_n denotes the predator population density at the n-th generation, p represents the predator's maximum food intake (consumption) rate, μ $(0<\mu<1)$ denotes the conversion efficiency from prey biomass to predator biomass, and m is the predator's mortality rate.

Further, we consider that prey uses vigilance as a survival strategy. So, our discrete-time predator-prey model with the vigilance of prey takes the following form:

$$\left\{ \begin{array}{lcl} x_{n+1} = & x_n \exp\left[\dfrac{r}{1+v}-d-\dfrac{ax_n}{1+v}-\dfrac{py_n}{k+v}\right], \\ y_{n+1} = & y_n \exp\left[\dfrac{\mu p x_n}{k+v}-m\right], \end{array} \right. \tag{1.3}$$

Here, $\frac{1}{k}$ is the lethality of the predator in the absence of vigilance, and v denotes the vigilance of the prey. As the strength of vigilance (v) increases, the predation pressure on prey decreases. On the other hand, the intraspecific competition among prey (a) and the birth rate of the prey (r) also decrease. In the model, vigilance

plays a positive role for prey as it reduces the predation pressure as well as the intra-specific competition but, on the negative side, it decreases the birth rate of prey population.

In Section 2 of this paper, we investigate the equilibria and give some logically valid parameter constraints. In Section 3, we study the stability and permanence of the fixed points. Both flip and Neimark-Sacker bifurcations are investigated in detail in Section 4. In Section 5, we present numerical simulations that illustrate the mathematical properties and give further insight into the bifurcation, attractors, and basins of attractions. Finally, we close the paper with a conclusion in which some unanswered mathematical questions are posed.

2. **Equilibria and parameter constraints.** In our model as given in Eq. (1.3), we have the parameters $r, d, a, p, m, k > 0, v \geq 0$ and $\mu \in (0, 1)$. In this section, we establish further sound constraints on the parameters. For our writing conveniences, we define

$$f_1(x) = \exp\left[\frac{(r-ax)}{1+v} - d\right],\ f_2(x) = \exp\left[\frac{\mu p x}{k+v} - m\right] \text{ and } g(y) = \exp\left[-\frac{py}{k+v}\right].$$

Thus, our model in System (1.3) becomes

$$\begin{cases} x_{n+1} = & x_n f_1(x_n) g(y_n), \\ y_{n+1} = & y_n f_2(x_n). \end{cases} \tag{2.1}$$

Let $\mathbb{R}^2_+ = \{(x, y) : \ x, y \geq 0\}$, and define $L : \ \mathbb{R}^2_+ \to \mathbb{R}^2_+$ as $L(x, y) = (xf_1(x)g(y), yf_2(x))$. Dynamics of Model (2.1) can be portrayed by the iterates of L. In the absence of a predator, the prey follows the well-known Ricker model [19], which has the trivial equilibrium $x = 0$, and the equilibrium $x^* = \frac{r}{a} - \frac{d}{a}(1 + v)$. The latter equilibrium is positive when $v < \frac{r}{d} - 1$. In our Model (2.1), we have the trivial equilibrium, $(0, 0)$, the predator-free equilibrium $(x^*, 0)$ and the coexistence equilibrium

$$(\bar{x}_2, \bar{y}_2) = \left(\frac{m(k+v)}{\mu p}, \frac{k+v}{p}\left[\frac{r\mu p - am(k+v)}{\mu p(1+v)} - d\right]\right).$$

Observe that $\bar{y}_2 > 0$ when

$$v < \frac{(r-d)\mu p - amk}{d\mu p + am}, \tag{2.2}$$

which can be assured when $\bar{x}_2 < x^*$. Fig. 1 illustrates the geometrical interplay between x^* and $\bar{x}_2, \bar{y}_2$. The next result establishes our first natural confinement on the parameters.

Proposition 1. *Consider the model in System (2.1). Each of the following holds true:*

- : *(i) If $v > \frac{r}{d} - 1$, then both, the prey and predator are doomed to extinction.*
- : *(ii) If $x^* < \frac{m}{a}(1 + v) < \bar{x}_2$, then the predator is doomed to extinction.*

Proof. (i) From the first equation in our model, we obtain $x_{n+1} < x_n$ for all $n \geq 0$. This implies $x_n \to 0$. From the second equation, there exists $N > 0$ such that $y_{n+1} < y_n$ for all $n > N$. Thus, $y_n \to 0$. To prove (ii), observe that $x^* < \frac{m}{a}(1 + v) < \bar{x}_2$,

implies $v > \dfrac{r}{m+d} - 1$ and $\dfrac{1+v}{k+v} < \dfrac{a}{\mu p}$. Now, write $x_{n+1}y_{n+1} = x_n y_n f_1(x_n) f_2(x_n)$ $g(y_n)$. Since the given conditions make

$$\frac{r}{1+v} - d - m < 0 \quad \text{and} \quad \frac{a}{1+v} - \frac{\mu p}{k+v} > 0,$$

we obtain $x_{n+1}y_{n+1} < x_n y_n$ for all values of n. Thus, $x_n y_n \to 0$. If $x_n \to 0$ or $y_n \to 0$, then we obtain the result. Otherwise, there must be a sequence n_k such that x_{n_k} goes to zero while y_{n_k} does not. From the first equation of the system, write

$$x_{n_k+2} \leq x_{n_k} \exp\left[\frac{2r}{1+v} - 2d\right],$$

then multiply both sides by y_{n_k} and take the limit for both sides to obtain $\lim x_{n_k+2}$ $y_{n_k} \to 0$. This can be done for any finite integer i to obtain $\lim x_{n_k+i} y_{n_k} \to 0$. But this contradicts the fact that $x_{j+1} > x_j$ when $x^* > 0$ and x_j is sufficiently small. The vector field in Fig. 1 illustrates this fact. Therefore, we must have $y_n \to 0$, and the proof is complete. □

It is natural to expect that x^* becomes positive before $\bar{y}_2$. Indeed, we stress this simple fact in the following proposition:

Proposition 2. *If $\bar{y}_2 > 0$, then $x^* > 0$.*

Proof. $x^* > 0$ if and only if $v < \frac{1}{d}(r-d)$, and $\bar{y}_2 > 0$ if and only if

$$v < \frac{1}{d + \frac{am}{\mu p}}(r-d) - \frac{akm}{d\mu p + am}.$$

The latter condition on v is stronger than the first one. Thus, $\bar{y}_2 > 0$ implies $x^* > 0$. □

Based on Proposition 1, we avoid the trivial dynamics, and directly proceed throughout this paper under the assumption $x^* > 0$, i.e., $v < \frac{r}{d} - 1$. Let c_1 be selected so that $t f_1(t) g(c_1 (f_2(t))^{-1}) \leq \bar{x}_2$ for all $t \geq 0$. This is possible because the expression is bounded in t and decreasing in c_1. Then define

$$M_1 := \max\{x f_1(x)\} = \frac{(1+v)}{a} \exp\left(\frac{r}{1+v} - d - 1\right),$$

$$\Omega_1 := \{(x,y) : \ 0 \leq y \leq c_1, 0 \leq x \leq \bar{x}_2\},$$

$$\Omega_\infty := \left\{(x,y) : \ x \geq 0, \ 0 \leq y \leq c_1 \exp[m - \frac{\mu p x}{k+v}]\right\}.$$

Furthermore, we add the following assumption on c_1 :

$$\max_{t \geq 0} t f_1(t) g\left(c(f_2(t))^{-1}\right) \leq f_2^{-1}\left(\frac{c_1}{c}\right) \quad \text{for all} \quad 0 < c \leq c_1. \tag{2.3}$$

Observe that when $c = c_1$, the right-hand-side is $\bar{x}_2$, and a loose bound on the left-hand-side can be $t f_1(t) g(c(f_2(t))^{-1}) \leq M_1 g(c(f_2(t))^{-1}) \leq M_1$. Now, we proceed to establish conditions in which Ω_1 and Ω_∞ are invariant sets. A set $B \subseteq \mathbb{R}^2_+$ is called positively invariant (or invariant for short) if $L(B) \subset B$.

Lemma 2.1. *Let $x^* > 0$. Each of the following holds true:*

(i) If $\bar{x}_2 \geq M_1$, then $L(\Omega_1) \subset \Omega_1$. Furthermore, the predator is doomed to extinction.

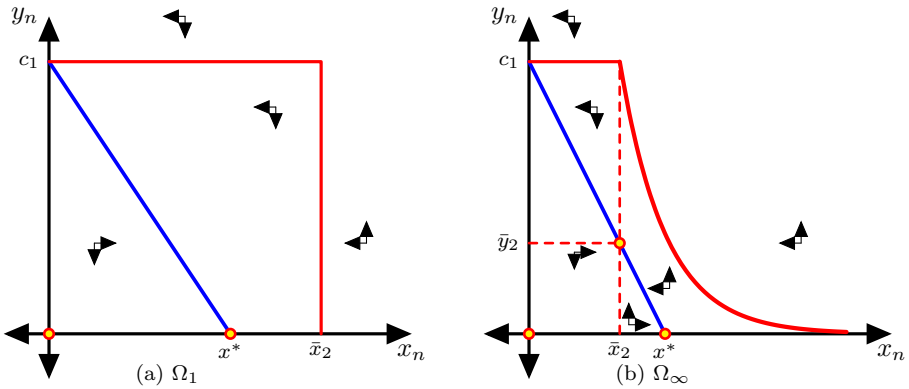

FIGURE 1. Figure (a) shows the region Ω_1 when $\bar{x}_2 \geq M_1$. Figure (b) shows the region Ω_∞ when $\bar{x}_2 < x^*$.

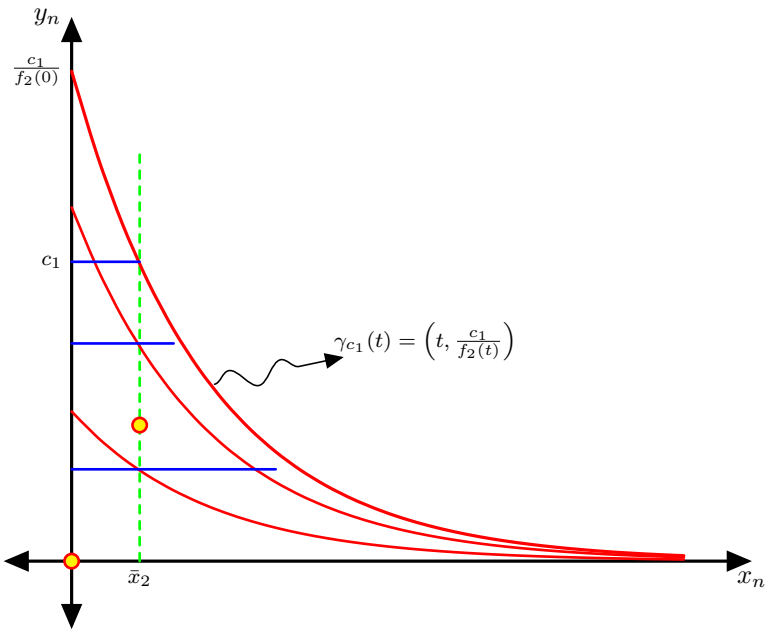

FIGURE 2. This figure shows the geometric illustration for establishing a positively invariant region. The top blue line segment represents $L(\gamma_{c_1}(t))$, while the two other blue line segments represent $L(\gamma_c(t))$ for two random choices of c.

(ii) If Condition (2.3) is satisfied, then $L(\Omega_\infty) \subset \Omega_\infty$.

Proof. Since $x^* \leq M_1$, it is obvious that $\bar{x}_2 \geq M_1$ implies $\bar{x}_2 > x^*$. Now, we verify Part (i). We show that $L(\Omega_1) \subseteq \Omega_1$. Since

$$\nabla(xf_1(x)g(y)) \quad \text{and} \quad \nabla(yf_2(x)) \neq (0,0),$$

the maximum of the two components of L take place on the boundary $\partial\Omega_1$. Thus, we test $L(\partial\Omega_1)$. $L(0,y) = (0, ye^{-m}) \in \partial\Omega_1$. $L(x,0) = (xf_1(x), 0) \in \partial\Omega_1$ due to the

fact $xf_1(x) \leq M_1$ and the condition $M_1 \leq \bar{x}_2$. $L(\bar{x}_2, y) = (\bar{x}_2 f_1(\bar{x}_2)g(y), y)$. Since

$$\bar{x}_2 f_1(\bar{x}_2)g(y) < \bar{x}_2 f_1(\bar{x}_2) < M_1 \leq \bar{x}_2 \quad \text{for all} \quad y \geq 0,$$

we obtain $L(\bar{x}_2, y) \in \Omega_1$ for all $0 \leq y \leq c_1$. Next, $L(x, c_1) = (xf_1(x)g(c_1), c_1 f_2(x))$. Since (x, c_1) is above the Nullcline of the first equation in System (2.1), we obtain

$$xf_1(x)g(c_1) \leq x \leq \bar{x}_2 \quad \text{and} \quad c_1 f_2(x) < c_1 f_2(\bar{x}_2) = c_1,$$

and consequently, $L(x, c_1) \in \partial\Omega_1$. Observe that $y_{n+1} \leq y_n$ for all $(x_n, y_n) \in \Omega_1$. This leads to $y_n \to 0$.

To prove Part (ii), we let $(s, t) \in \Omega_\infty$ and show that $L(s, t) \in \Omega_\infty$. If (s, t) belongs to one of the axes, then it follows from part (i). Let $(s, t) \in \Omega_\infty$ without the axes. The point (s, t) can be interpolated by a curve of the form $\gamma_c(t)$ for some $t > 0$ and $0 < c \leq c_1$. Thus, we focus on $L(\gamma_c(t))$ for all $t > 0$ and $0 < c \leq c_1$. We have

$$L(\gamma_c(t)) = \left(tf_1(t)g\left(\frac{c}{f_2(t)}\right), c \right),$$

which is a horizontal line segment of finite length. As illustrated in Fig. 2, all we need is to guarantee that $L(\gamma_c(t))$ does not bypass the upper curve $\gamma_{c_1}(t)$, i.e.,

$$tf_1(t)g\left(\frac{c}{f_2(t)}\right) \leq f_2^{-1}\left(\frac{c_1}{c}\right)$$

for all $t > 0$ and $0 < c \leq c_1$. By our choice of c_1 and Condition (2.3), the proof is complete. □

We close this section by discussing the notion of dissipation [6]. System (2.1) (or equivalently the map L) is called point dissipative if it is ultimately bounded, i.e., if there is a bounded set B such that for all $(x_0, y_0) \in \mathbb{R}^2_+$, there exists $N > 0$ in which $L^n(x_0, y_0) \in B$ for all $n > N$. The system is called bounded dissipative if B attracts every bounded set in $\mathbb{R}^2_+$. Because $\mathbb{R}^2_+$ is locally compact, then bounded dissipative is equivalent to point dissipative. Based on Lemma 2.1, we have the following result.

Theorem 2.2. *Let $x^* > 0$, and assume that $\bar{x}_2 \geq M_1$. System (2.1) is bounded dissipative.*

Proof. Obviously, for all values of the parameters, the prey is bounded from the first equation, i.e., for all $(x_0, y_0) \in \mathbb{R}^2_+$, $x_n \leq M_1$ for all $n \geq 1$. The predator is bounded as a consequence of the results obtained in Lemma 2.1. □

3. Stability and permanence.

In this section, we discuss the local stability of the equilibria, verify the existence of a global attractor, and show permanence (uniform persistence) [1]. Throughout this paper, we equip $\mathbb{R}^2_+$ with the Euclidean metric $\|\cdot\|$, and the distance $d(\cdot)$ between points, sets, or a point and a set is defined as usual. We start with local stability.

3.1. Local stability.

A nonempty invariant subset B of $\mathbb{R}^2_+$ is called locally stable if any neighborhood V of B contains a neighborhood U such that $L(U) \subset V$. B is called attracting set if there exists a neighborhood V of B such that $\lim(d(B, L^n(V))) = 0$ as $n \to \infty$. B is called locally asymptotically stable (LAS) if it is locally stable and attractive. Here, our interest of B is limited to the equilibrium points, and in this case, the eigenvalues of the linearized system are good tools to characterized local asymptotic stability. Recall that Model (2.1) has the

trivial equilibrium $(0,0)$, the predator-free equilibrium $(x^*,0)$ and the coexistence equilibrium $(\bar{x}_2,\bar{y}_2)$. At an equilibrium point $(\bar{x},\bar{y})$, the Jacobian matrix

$$J(\bar{x},\bar{y}) = \begin{bmatrix} (\bar{x}f_1'(\bar{x}) + f_1(\bar{x}))g(\bar{y}) & (\bar{x}f_1(\bar{x}))g'(\bar{y}) \\ \bar{y}f_2'(\bar{x}) & f_2(\bar{x}) \end{bmatrix}$$

has eigenvalues λ_1 and λ_2 that satisfy

$$\lambda_1 + \lambda_2 = Tr(J) \quad \text{and} \quad \lambda_1\lambda_2 = Det(J).$$

At $(\bar{x},\bar{y}) = (0,0)$, we obtain

$$\lambda_1(0,0) = \exp\left(\frac{r}{1+v} - d\right) \quad \text{and} \quad \lambda_2(0,0) = e^{-m}.$$

Under our parameter constraints, we have $\lambda_1(0,0) > 1$ and $\lambda_2(0,0) < 1$. At $(\bar{x},\bar{y}) = (x^*,0)$, we obtain

$$\begin{aligned} \lambda_1(x^*,0) =& 1 - \frac{ax^*}{1+v} = d + 1 - \frac{r}{1+v} \\ \lambda_2(x^*,0) =& \exp\left(\frac{\mu p x^*}{(k+v)} - m\right) \\ =& \exp\left(\frac{\mu p(r - d(1+v))}{a(k+v)} - m\right). \end{aligned}$$

At $(\bar{x},\bar{y}) = (\bar{x}_2,\bar{y}_2)$, we obtain

$$J(\bar{x}_2,\bar{y}_2) = \begin{bmatrix} 1 - \frac{a\bar{x}_2}{1+v} & -\frac{p\bar{x}_2}{k+v} \\ \frac{p\mu\bar{y}_2}{k+v} & 1 \end{bmatrix}.$$

The trace and determinant are given by

$$T := Tr(J(\bar{x}_2,\bar{y}_2)) = 2 - \frac{a\bar{x}_2}{1+v} = 2 - \frac{am}{\mu p}\frac{k+v}{1+v} \tag{3.1}$$

and

$$\begin{aligned} D := Det(\bar{x}_2,\bar{y}_2) =& 1 - \frac{a\bar{x}_2}{1+v} + \frac{\mu p^2}{(k+v)^2}\bar{x}_2\bar{y}_2 \\ =& 1 - \frac{a}{1+v}\bar{x}_2 + \frac{mp}{(k+v)}\bar{y}_2. \end{aligned} \tag{3.2}$$

Local stability of two dimensional systems can be classified based on the following lemma [2].

Lemma 3.1 ([2]). *Let $(\bar{x},\bar{y})$ be an equilibrium solution of a two dimensional discrete system. If T is the trace and D is the determinant of the Jacobian matrix at $(\bar{x},\bar{y})$, then each of the following holds true:*

(i) $(\bar{x},\bar{y})$ is a sink if

$$-1 < D < 1 \quad \textit{and} \quad -D - 1 < T < D + 1.$$

(ii) $(\bar{x},\bar{y})$ is a source if

$$D > 1 \quad \textit{and} \quad -D - 1 < T < D + 1, \ \textit{or} \quad D < -1 \quad \textit{and} \quad D + 1 < T < -D - 1.$$

(iii) $(\bar{x},\bar{y})$ is a saddle if $|D+1| < |T|$.

(iv) $(\bar{x},\bar{y})$ is non-hyperbolic if

$$|T| = |D+1|, \quad \textit{or} \quad D = 1 \quad \textit{and} \quad |T| \le 2.$$

Denote $X := \frac{a}{1+v}\bar{x}_2$ and $Y := \frac{mp}{k+v}\bar{y}_2$, then $D > -1$ translates into $Y > X - 2$, $D < 1$ translates into $Y < X$, $T > -D - 1$ translates into $Y > 2X - 4$, and $T < D + 1$ translates into $Y + 2 > 2$, which is always satisfied. Therefore, Lemma 3.1 can be deciphered based on the values of X and Y in Figure 3.

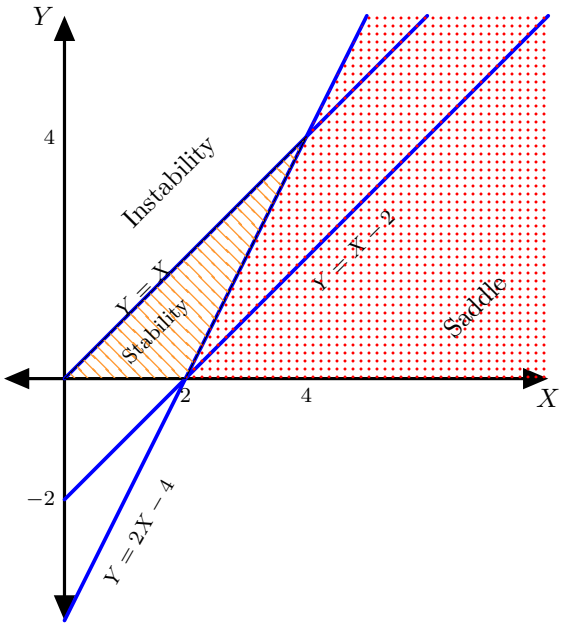

FIGURE 3. This figure illustrates the stability scenarios of the coexistence equilibrium $(\bar{x}_2, \bar{y}_2)$ based on Lemma 3.1 and the values of $X := \frac{a}{1+v}\bar{x}_2$, $Y := \frac{mp}{k+v}\bar{y}_2$. The shaded dashed-region reflects the local stability region of the coexistence equilibrium.

Now, we depend on Lemma 3.1 and its illustration in Fig. 3 to characterize local stability of the equilibria in System 2.1. For our writing convenience, we define

$$\gamma := \frac{4\mu p}{m}, \quad \alpha := \mu p(r-d) - ak(m+1), \qquad \beta := d\mu p + a(m+1),$$

$$v_0 := \min\left\{\frac{r}{d+2} - 1, \frac{\alpha + ak}{\beta - a}\right\} \quad \text{and} \quad v_1 := \max\left\{\frac{r}{d+2} - 1, \frac{\alpha + ak}{\beta - a}\right\}.$$

Theorem 3.2. *Consider $x^* > 0$. Each of the following holds true.*

(i) The trivial equilibrium $(0,0)$ is a saddle, and its stable manifold is the positive y-axis.

(ii) The predator free equilibrium $(x^*, 0)$ is stable when $v > v_1$, and it is unstable when $v < v_0$. $(x^*, 0)$ is a saddle with a stable manifold along the positive x-axis when v between v_0 and v_1.

(iii) Assume $\bar{x}_2 < x^*$. $(\bar{x}_2, \bar{y}_2)$ is locally asymptotically stable if

$$\alpha < v\beta \quad \text{and} \quad (\beta + a - \gamma)v < \gamma + \alpha - ak,$$

unstable if

$$v\beta < \alpha \quad \text{and} \quad (\beta + a - \gamma)v < \gamma + \alpha - ak,$$

and a saddle if $(\beta + a - \gamma)v > \gamma + \alpha - ak$.

Proof. Part (i) is obvious. Part (ii) follows straightforward from the eigenvalues $\lambda_1(x^*, 0)$ and $\lambda_2(x^*, 0)$. $-1 < \lambda_1(x^*, 0) < 1$ when $v > \frac{r}{d+2} - 1$, and $\lambda_1(x^*, 0) < -1$ when $v < \frac{r}{d+2} - 1$. $0 < \lambda_2(x^*, 0) < 1$ when $v(\beta - a) > \alpha + ak$, which is

$$v > \frac{\mu p(r - d) - akm}{d\mu p + am} \qquad \text{(equivalently } \bar{x}_2 > x^*\text{)}.$$

$\lambda_2(x^*, 0) > 1$ when $\bar{x}_2 < x^*$. Thus, $(x^*, 0)$ is stable when $v > v_1$, and it is unstable when $v < v_0$. The saddle case becomes obvious. Next, we prove Part (iii). Observe that $Y > 0$ guarantees the existence of the coexistence equilibrium $(\bar{x}_2, \bar{y}_2)$, which is assured by $\bar{x}_2 < x^*$. This is equivalent to the condition in Inequality (2.2), i.e, $v < \frac{\alpha + ak}{\beta - a}$. Now, the local stability is assured by $2X - 4 < Y < X$ in Fig. 3. $Y < X$ is equivalent to $v > \frac{\alpha}{\beta}$, and $Y > 2X - 4$ is equivalent to

$$(\beta + a - \gamma)v < \gamma + \alpha - ak.$$

The rest of the proof goes through the same idea. In particular $Y > X$ and $Y > 2X - 4$ make $(\bar{x}_2, \bar{y}_2)$ unstable, which is equivalent to the inequalities $v\beta < \alpha$ and $(\beta + a - \gamma)v < \gamma + \alpha - ak$. The saddle case is obtainable when $Y < 2X - 4$, which is equivalent to $(\beta + a - \gamma)v > \gamma + \alpha - ak$. □

From Theorem 3.2 and Figure 1, $\bar{y}_2 > 0 \quad \Leftrightarrow \quad \bar{x}_2 < x^* \quad \Leftrightarrow \quad \lambda_2(x^*, 0) > 1$. Therefore, bi-stability in the steady states is not a viable scenario.

3.2. **Global stability and permanence.** We start by stressing some needed concepts. A nonempty, compact, and invariant set $B \subset \mathbb{R}^2_+$ is called an attractor of System (2.1) if there exists a neighborhood U of B such that $\lim(d(B, L^n(U))) = 0$ as $n \to \infty$. B is called a global attractor if $\lim(d(B, L^n(U))) = 0$ as $n \to \infty$, where $U = \mathbb{R}^2_+ \setminus \{(x, 0), (0, y) : \ x, y \geq 0\}$. System (2.1) is called asymptotically smooth if for any nonempty compact subset of $\mathbb{R}^2_+$ for which $T(B) \subset B$, there is a compact set $J \subset B$ such that J attracts B. A species is called persistent if it starts finite, stays finite, and does not come arbitrarily close to zero. A species is called permanent (or uniformly persistent) if it starts finite, and eventually enters a compact subset of $\mathbb{R}^+$. In the predator-free model, the local stability of the equilibrium x^* implies its global stability with respect to the interval $(0, \infty)$. When the predator is introduced in the model, the equilibrium $(x^*, 0)$ is expected to inherit the global stability for a certain range of the parameters. Indeed, we have the following result.

Proposition 3. *If* $0 < x^* \leq \bar{x}_2$ *and* $v \geq \frac{r}{d+1} - 1$, *then the predator free equilibrium* $(x^*, 0)$ *is globally asymptotically stable.*

Proof. From the first equation in Model (2.1), we have $x_{n+1} \leq x_n f_1(x_n)$. The condition $v \geq \frac{r}{d+1} - 1$ makes the convergence in $x_n f_1(x_n)$ to be eventually monotonic. Therefore, we obtain $\limsup x_n \leq x^*$. There exists $n_1 \in \mathbb{N}$ such that $x_n \leq x^*$ for all $n \geq n_1$. Consequently, since $x^* \leq \bar{x}_2$, there exists $n_2 \in \mathbb{N}$ such that

$$y_{n+1} \leq y_n f_2(x^*) \leq y_n f_2(\bar{x}_2) = y_n \quad \text{for all} \quad n \geq n_2.$$

Thus, $\{y_n\}$ is eventually decreasing, and consequently must converge to a fixed point. Hence, the predator goes extinct, and $(x^*, 0)$ is globally asymptotically stable. □

The continuous map $L : \mathbb{R}^2_+ \to \mathbb{R}^2_+$ is called completely continuous if for any bounded subset $B \subset \mathbb{R}^2_+$, $\overline{L(B)}$ is compact. Obviously, L is completely continuous. It is well-known that completely continuous maps are asymptotically smooth [6, 24]. Now, we cite the following theorem from [5] (see also [24], theorems 1.1.2 and 1.1.3), which helps us to verify the existence of a global attractor.

Theorem 3.3. *Let X be a complete metric space, and suppose that $F : X \to X$ is completely continuous. If F is point dissipative on X, then there is a global attractor for F.*

Based on Theorem 3.3 and Theorem 2.2, we obtain a global attractor that includes the coexistence equilibrium.

Corollary 1. *Let $x^* > 0$, and assume that Condition 2.3 is satisfied, then System (2.1) has a global attractor.*

From the invariant sets obtained in Section 2, it is obvious that both the predator and prey eventually enter a compact set. To test their permanence, it remains to find conditions under which they stay away from collapsing to zero.

Proposition 4. *Assume $v < \frac{r}{d} - 1$. The prey is permanent.*

Proof. Since x_n becomes smaller than $M_1 = \max\{xf_1(x)\}$ in finite time, it remains to show that x_n stays away from zero. From the invariant sets obtained in Lemma 2.1, there exists $n_0 \geq 0$ such that $y_n < c_1$ for all $n > n_0$. Thus, for $n > n_0$, we obtain

$$\begin{aligned} x_{n+1} &> x_n f_1(x_n) g(c_1) \\ &= x_n \exp\left[\frac{-ax_n}{1+v}\right]. \end{aligned}$$

From the fact that $v < \frac{r}{d} - 1$ and $x_n \leq M_1$, there exists $N > n_0$ such that

$$x_n \geq M_1 \exp\left[\frac{-aM_1}{1+v}\right] \quad \text{for all} \quad n > N.$$

Hence, the prey is permanent. □

Next, we assume the equilibrium $(x^*, 0)$ to be unstable, and depend on the technique developed by Hofbauer and So [7] to show that System (2.1) is permanent. To familiarize the reader with the used concepts, we give the definition of an isolated invariant set. A compact invariant subset M of $\mathbb{R}^2_+$ is called isolated if there exists a closed neighborhood U of M for which M is the largest invariant set.

Theorem 3.4. [7] *Let X be a metric space and $F : X \to X$ be continuous. Assume that Y is closed in X such that $X \setminus Y$ is positively invariant. Suppose B is a global attractor in X, M is the maximal compact invariant set in Y such that M is isolated in B. If the stable set of M is contained in Y, then F is permanent.*

Theorem 3.5. *Assume $v < v_0$, then System (2.1) is permanent.*

Proof. Assume $v < v_0$, and recall from Theorem 3.2 and its proof that for $0 < \bar{x}_2 < x^*$, $(x^*, 0)$ is unstable and $(0, 0)$ is a saddle. Furthermore, $Y := \{(x, y) : xy = 0 \quad \text{and} \quad x, y \geq 0\}$ is closed in $\mathbb{R}^2_+$ and $L(\mathbb{R}^2_+ \setminus Y) \subset \mathbb{R}^2_+ \setminus Y$. Define $M := \{(0, 0), (x^*, 0)\}$, then M is the maximal compact invariant set in Y. The condition $v < v_0$ makes $\bar{x}_2 < x^*$, and the vector field illustrated in Part (b) of Fig. 1 shows that M is isolated. Finally, it is obvious that $L(Y) = Y$, which means the stable set of M is contained in Y. Therefore, System (2.1) is permanent by Theorem 3.4. □

4. **Bifurcation analysis.** Let the condition in Inequality (2.2) continue to hold (i.e., $\bar{x}_2 < x^*$). If $D = 1$ and $-2 < T < 2$, System 2.1 is expected to go through a Neimark-Sacker (Hopf) bifurcation. This means $Y = X$ and $0 \leq X < 4$ in Fig. 3. We consider the vigilance v as the bifurcation parameter to obtain

$$v = v^* := \frac{\mu p(r-d) - ak(m+1)}{a(m+1) + d\mu p} \quad \text{and} \quad \frac{k+v}{1+v} < \frac{4\mu p}{am}.$$

Observe that v^* is positive when $\mu p(r-d) > ak(m+1)$. This condition is stronger than the condition in Inequality (2.2), which guarantees the existence of the coexistence equilibrium. We stress some facts in the following simple proposition, then give the Neimark-Sacker bifurcation theorem.

Proposition 5. *Define $q(v) = \frac{a\bar{x}_2}{1+v}$ and assume $r > \frac{ak}{\mu p}(m+1) + d$. Each of the following holds true.*

(i) $v^* > 0$ *and* $\bar{x}_2 < x^*$
(ii) $k \neq 1$
(iii) $q := q(v^*) \neq \frac{am}{\mu p}$.

Proof. (i) When $r > \frac{ak}{\mu p}(m+1) + d$, we obtain $(r-d)\mu p - amk > 0$ and

$$0 < v^* < \frac{(r-d)\mu p - amk}{d\mu p + am}.$$

Also, from Inequality (2.2), $(\bar{x}_2, \bar{y}_2)$ exists as a coexistence equilibrium which means $\bar{x}_2 < x^*$. To prove Part (ii), substitute $v = v^*$ and $\bar{x}_2 = \frac{m(k+v^*)}{\mu p}$ in q, then solve for v^* to obtain

$$v^* = \frac{\mu pq - akm}{am - \mu pq}. \tag{4.1}$$

Since $v^* > 0$ by Part (i), we must have $k \neq 1$. Finally, $k \neq 1$ forces q to be different from $\frac{am}{\mu p}$ which completes the proof of Part (iii). □

Theorem 4.1. *Consider System (2.1), define q as in Proposition 5 and assume $\mu pr > \mu pd + ak(m+1)$. If*

$$\frac{k+v^*}{1+v^*} < \frac{4\mu p}{am}, \qquad r \neq \frac{a(m+1)(k-1)}{\mu p}, \frac{a(k-1)(m(d+j)+j)}{jp\mu - am},\ j = 2,3,4,$$

and $q^3 - 4q^2 + 4mq + 8m^2 \neq 0$, then the coexistence equilibrium $(\bar{x}_2, \bar{y}_2)$ goes through a Neimark-Sacker bifurcation at $v = v^*$.

Proof. The non-hyperbolicity condition is satisfied at $v = v^*$ since we obtain two complex eigenvalues $\lambda_i, i = 1, 2$ with modulus one. Next, we check the transversality condition $\frac{d}{dv}|\lambda_i(v^*)| \neq 0$ and the non-strong resonance condition $\lambda_i^j(v^*) \neq 1$ for $j = 1, 2, 3, 4$. Since

$$|\lambda_i(v)| = \sqrt{D(v)}, \quad \text{we obtain} \quad \frac{d}{dv}|\lambda_i(v)| = \frac{D'(v)}{2\sqrt{D(v)}}$$

and

$$D'(v) = \frac{m}{\mu p}\frac{(ak(m+1) - \mu pr - a(m+1))}{(1+v)^2},$$

Thus,

$$r \neq \frac{a(m+1)(k-1)}{\mu p} \quad \text{ensures that} \quad \frac{d}{dv}|\lambda_i(v^*)| \neq 0.$$

Now, we test $\lambda_i^j(v^*) = 1$. At $j = 1, \lambda_i(v^*) = 1$ if and only if $T = 2$, which is not possible since $T = 2 - \frac{a\bar{x}_2}{1+v}$. When $j = 2, \lambda_i^2(v^*) = 1$ if and only if $T = 2$ or -2. We are done with $T = 2$. $T = -2$ when $\bar{x}_2 = \frac{4(1+v)}{a}$. The condition

$$r \neq \frac{a(k-1)(m(d+4)+4)}{4p\mu - am} \quad \text{ensures that} \quad \bar{x}_2 \neq \frac{4(1+v)}{a} \quad \text{at} \quad v = v^*.$$

When $j = 3$ or 4, $\lambda_i^j(v^*) = 1$ if and only if $T = 2, -1, -1$ or $2, -2, 0, 0$. Thus, it remains to show that $(T, D) = (0, 1)$ or $(-1, 1)$ is not possible at $v = v^*$. From the expression of T in Eq. (3.1), we need to show that

$$q(v) = \frac{a\bar{x}_2}{1+v} \neq 2, 3 \quad \text{at} \quad v = v^*.$$

This is ensured by the condition

$$r \neq \frac{a(k-1)(m(d+j)+j)}{jp\mu - am} \quad \text{for} \quad j = 2, 3.$$

Finally, it remains to verify the nondegeneracy condition. Since at $v = v^*$, the eigenvalues of the Jacobian matrix are on the unit circle, we depend on Eqs (3.1) and (3.2) to obtain

$$J(\bar{x}_2, \bar{y}_2) = \begin{bmatrix} 1-q & -\frac{m}{\mu} \\ \frac{\mu}{m}q & 1 \end{bmatrix},$$

where $q = q(v^*)$ as defined in Proposition 5. Obviously, $(T, D) = (2-q, 1)$ and the eigenvalues are $\lambda = 1 - \frac{1}{2}q + \frac{1}{2}\sqrt{q(4-q)}i$ together with its conjugate. It is worth stressing that $q < 4$ is equivalent to $\frac{k+v^*}{1+v^*} < \frac{4\mu p}{am}$. Next, shift the equilibrium point $(\bar{x}_2, \bar{y}_2)$ to make it at the origin, i.e., let $(U_n, V_n) = (x_n - \bar{x}_2, y_n - \bar{y}_2)$. We obtain

$$\begin{cases} U_{n+1} = & F_1(U_n, V_n) := (U_n + \bar{x}_2) f_1(U_n + \bar{x}_2) g(V_n + \bar{y}_2) - \bar{x}_2 \\ V_{n+1} = & G_1(U_n, V_n) := (V_n + \bar{y}_2) f_2(U_n + \bar{x}_2) - \bar{y}_2. \end{cases} \tag{4.2}$$

Since $q = \frac{a\bar{x}_2}{1+v} = \frac{mp\bar{y}_2}{k+v}$ at $v = v^*$, we write $\bar{x}_2$ and $\bar{y}_2$ in terms of q. Then we take the Taylor expansion of the right hand side in System (4.2) at the origin. We obtain

$$\begin{bmatrix} U_{n+1} \\ V_{n+1} \end{bmatrix} = \begin{bmatrix} 1-q & -\frac{m}{\mu} \\ \frac{\mu}{m}q & 1 \end{bmatrix} \begin{bmatrix} U_n \\ V_n \end{bmatrix} + \begin{bmatrix} F_2(U_n, V_n) \\ G_2(U_n, V_n) \end{bmatrix} + \begin{bmatrix} \mathcal{O}(|U_n, V_n|^4) \\ \mathcal{O}(|U_n, V_n|^4) \end{bmatrix},$$

where

$$\begin{aligned} F_2(U, V) =& \frac{a(q-2)}{2(1+v)}U^2 + \frac{p(q-1)}{k+v}UV + \frac{p^2q(1+v)}{2a(k+v)^2}V^2 + \frac{a^2(3-q)}{6(1+v)^2}U^3 \\ &+ \frac{p^2(1-q)}{2(k+v)^2}UV^2 + \frac{ap(2-q)}{2(1+v)(k+v)}VU^2 - \frac{p^3q(1+v)}{6a(k+v)^3}V^3 \end{aligned}$$

and $G_2(U, V) =$

$$\frac{p\mu^2 q}{2m(k+v)}U^2 + \frac{\mu p}{k+v}UV + 0V^2 + \frac{p^2q\mu^3}{6m(k+v)^2}U^3 + 0UV^2 + \frac{\mu^2p^2}{2(k+v)^2}VU^2 + 0V^3.$$

To transform the Jacobian matrix into the Jordan normal form $S^{-1}JS$, consider the transformation

$$\begin{bmatrix} U \\ V \end{bmatrix} = S \begin{bmatrix} X \\ Y \end{bmatrix}, \quad \text{where} \quad S = \begin{bmatrix} 0 & m \\ -\frac{\mu}{2}\sqrt{q(4-q)} & -\frac{\mu q}{2} \end{bmatrix}.$$

To avoid massive expressions in the coefficients, we find it convenient to write v^* in terms of q as given in Eq. (4.1). Thus, we obtain

$$\begin{bmatrix} X_{n+1} \\ Y_{n+1} \end{bmatrix} = \begin{bmatrix} 1-\frac{q}{2} & -\frac{1}{2}\sqrt{q(4-q)} \\ \frac{1}{2}\sqrt{q(4-q)} & 1-\frac{q}{2} \end{bmatrix} \begin{bmatrix} X_n \\ Y_n \end{bmatrix} + \begin{bmatrix} F_3(X_n,Y_n) \\ G_3(X_n,Y_n) \end{bmatrix} + \begin{bmatrix} \mathcal{O}(|X_n,Y_n|^4) \\ \mathcal{O}(|X_n,Y_n|^4) \end{bmatrix},$$

where

$$F_3(X,Y) = \frac{(am-\mu pq)}{(k-1)}\left(a_1X^2 + a_2XY + a_3Y^2 + a_4X^3 + a_5XY^2 + a_6X^2Y + a_7Y^3\right),$$

$$a_1 := \tfrac{1}{8}\sqrt{q(4-q)}, \qquad a_2 := \tfrac{(2q-4m-q^2)}{4q}, \qquad a_3 := -a_1,$$

$$a_4 := \tfrac{(q-4)(am-\mu pq)}{48(k-1)}, \quad a_5 := \tfrac{(am-\mu pq)(8m^2+4q^2-q^3)}{16q^2(k-1)}, \quad a_6 := \tfrac{(q-2)\sqrt{q(4-q)}(am-\mu pq)}{16q(k-1)},$$

$$a_7 := \tfrac{(am-\mu pq)(q^3+8m^2-6q^2)}{48q(k-1)\sqrt{q(4-q)}},$$

and

$$G_3(X,Y) = \frac{(am-\mu pq)}{(k-1)}\left(b_1X^2 + b_2XY + b_3Y^2 + b_4X^3 + b_5XY^2 + b_6X^2Y + b_7Y^3\right),$$

$$b_1 := \tfrac{1}{8}(q-4), \qquad b_2 := \tfrac{(q-2)\sqrt{q(4-q)}}{4q}, \qquad b_3 := -b_1,$$

$$b_4 := \tfrac{(4-q)^2(am-\mu pq)}{48(k-1)\sqrt{q(4-q)}}, \quad b_5 := \tfrac{(am-\mu pq)(q-4)\sqrt{q(4-q)}}{16q(k-1)}, \quad b_6 := \tfrac{(q-2)(q-4)(am-\mu pq)}{16q(k-1)},$$

$$b_7 := \tfrac{(am-\mu pq)(6-q)}{48(k-1)}.$$

Next, we evaluate

$$\eta = -Re\left(\frac{(1-2\lambda)\bar{\lambda}^2}{1-\lambda}C_{11}C_{20}\right) - \frac{1}{2}|C_{11}|^2 - |C_{02}|^2 + Re\left(\bar{\lambda}C_{21}\right), \tag{4.3}$$

where

$$\begin{aligned} C_{11} :=& \frac{1}{4}\left(F_{3XX} + F_{3YY} + i\left(G_{3XX} + G_{3YY}\right)\right) \\ C_{20} :=& \frac{1}{8}\left(F_{3XX} - F_{3YY} + 2G_{3XY} + i\left(G_{3XX} - G_{3YY} - 2F_{3XY}\right)\right) \\ C_{02} :=& \frac{1}{8}\left(F_{3XX} - F_{3YY} - 2G_{3XY} + i\left(G_{3XX} - G_{3YY} + 2F_{3XY}\right)\right) \\ C_{21} :=& \frac{1}{16}\left(F_{3XXX} - F_{3XYY} + G_{3XXY} + G_{3YYY}\right. \\ & \left. + i\left(G_{3XXX} - G_{3XYY} - F_{3XXY} - F_{3YYY}\right)\right) \end{aligned}$$

are evaluated at $(X,Y) = (0,0)$ and $v = v^*$. It is a matter of lengthy but straightforward computations to find

$$\eta = -\frac{(am-\mu pq)^2(q^3+8m^2+4mq-4q^2)}{64q^2(k-1)^2}.$$

From Proposition 5, neither $k = 1$ nor $am = pq\mu$. Thus $\eta \neq 0$ when $q^3 + 8m^2 + 4mq - 4q^2 \neq 0$ which completes the proof. □

For more details about the normal form and nondegenerate conditions of Neimark-Sacker bifurcation, we refer readers to the work of Huang et al [8].

Our next example illustrates and validates the above results.

Example 4.2. Consider the model in System (1.3), and fix

$$d = \frac{1}{10},\ p = 1,\ k = 5,\ \mu = \frac{7}{10},\ m = \frac{3}{10}, a = \frac{1}{5}.$$

In this case, we obtain

$$x^* = \frac{1}{2}\left(10r - v - 1\right), \bar{x}_2 = \frac{1}{7}\left(15 + 3v\right), \quad \text{and} \quad \bar{y}_2 = \frac{(5+v)(70r - 13v - 37)}{70(1+v)}.$$

To have $x^* > 0$, we need $v < 10r - 1$, and to have $\bar{x}_2 < x^*$, we need $v < \frac{1}{13}(70r - 37)$. Therefore, we need $r > \frac{37}{70}$ and $v < \frac{1}{13}(70r - 37)$. Next, we have $v^* = \frac{1}{33}(70r - 137)$, which is positive when $r > \frac{137}{70}$. The parameter values of this example will be considered in our numerical simulations in the next section.

Next, we proceed to investigate period-doubling bifurcation. A period doubling bifurcation occurs when $D + T + 1 = 0$ and $-2 < T < 0$. These two conditions give us

$$v = \tilde{v} := \frac{\gamma + \alpha - ak}{\beta + a - \gamma} \quad \text{and} \quad \frac{2\mu p}{am} < \frac{k+v}{1+v} < 4\frac{\mu p}{am}.$$

We use the center manifold reduction to test the super-criticality of the 2-cycle obtained after the bifurcation. As in System (4.2), shift the equilibrium point $(\bar{x}_2, \bar{y}_2)$ to make it at the origin, i.e., let $(u_n, v_n) = (x_n - \bar{x}_2, y_n - \bar{y}_2)$ to obtain

$$\begin{cases} u_{n+1} = & F_1(u_n, v_n) := (u_n + \bar{x}_2) f_1(u_n + \bar{x}_2) g(v_n + \bar{y}_2) - \bar{x}_2 \\ v_{n+1} = & F_2(u_n, v_n) := (v_n + \bar{y}_2) f_2(u_n + \bar{x}_2) - \bar{y}_2. \end{cases} \tag{4.4}$$

We follow the notations of Kuznetsov [10] (Chapter 4). Let q be the eigenvector that belongs to the eigenvalue $\lambda_1 = -1$, and let p be the adjoint eigenvector, i.e., $J(0,0)q = \lambda_1 q$ and $J^T((0,0))p = \lambda_1 p$, respectively ($J(0,0)$ after the shift is the same as $J(\bar{x}_2, \bar{x}_2)$ before the shift). We normalize p and q with respect to the Euclidean inner product, i .e., $< p, q >= 1$. The normal form becomes

$$\xi \ \mapsto \ -\xi + \frac{1}{6}c\xi^3 + O(\xi^4),$$

where $c :=< p, C(q,q,q) > -3 < p, B(q, (J - I_2)^{-1} B(q,q)) >$,

$$B(q,q) = \begin{bmatrix} B_1(q_1, q_2) \\ B_2(q_1, q_2) \end{bmatrix}, \quad C(q,q,q) = \begin{bmatrix} C_1(q_1, q_2) \\ C_2(q_1, q_2) \end{bmatrix}$$

and

$$B_i(q_1, q_2) = \frac{\partial^2 F_i(0,0)}{\partial x^2} q_1^2 + 2\frac{\partial^2 F_i(0,0)}{\partial xy} q_1 q_2 + \frac{\partial^2 F_i(0,0)}{\partial y^2} q_2^2$$

$$C_i(q_1, q_2) = \frac{\partial^3 F_i(0,0)}{\partial x^3} q_1^3 + 3\frac{\partial^3 F_i(0,0)}{\partial x^2 \partial y} q_1^2 q_2 + 3\frac{\partial^3 F_i(0,0)}{\partial y^2 \partial x} q_1 q_2^2 + \frac{\partial^3 F_i(0,0)}{\partial y^3} q_2^3.$$

At $v = \tilde{v}$, write $\lambda_1 = -1$ and $\lambda_2 = \lambda$, then $J(0,0)$ becomes

$$J := \begin{bmatrix} \lambda - 2 & -\frac{m}{\mu} \\ \frac{2\mu}{m}(1 - \lambda) & 1 \end{bmatrix}. \tag{4.5}$$

We consider eigenvectors p and q after normalization with respect to the Euclidian inner product as

$$p = \begin{bmatrix} p_1 \\ p_2 \end{bmatrix} = \frac{1}{\lambda+1}\begin{bmatrix} \frac{2\mu}{m} \\ 1 \end{bmatrix} \quad q = \begin{bmatrix} q_1 \\ q_2 \end{bmatrix} = \frac{1}{\lambda+1}\begin{bmatrix} \frac{m}{\mu} \\ \lambda-1 \end{bmatrix}.$$

Next, we use a CAS to do the computations. We evaluate $B(q,q)$ and $C(q,q,q)$ to obtain

$$B_1(q_1,q_2) = \frac{m[(p\mu(\lambda-1)(\tilde{v}+1)+am(\tilde{v}+k)][(p\mu(\lambda-3)(\tilde{v}+1)+am(\tilde{v}+k)]}{\mu^3 p(1+\tilde{v})^2(k+\tilde{v})}$$

$$B_2(q_1,q_2) = -\frac{m[p\mu(dm-2\lambda+2)(\tilde{v}+1)+am^2(\tilde{v}+k)-pmr\mu]}{\mu(k+\tilde{v})(1+\tilde{v})}$$

and

$$C_1(q_1,q_2) = -\frac{m[p\mu(\lambda-4)(\tilde{v}+1)+am(\tilde{v}+k)][p\mu(\lambda-1)(\tilde{v}+1)+am(\tilde{v}+k)]^2}{(\mu^4 p(1+\tilde{v})^3(k+\tilde{v})^2)}$$

$$C_2(q_1,q_2) = -\frac{pm^2[p\mu(dm-3\lambda+3)(\tilde{v}+1)+am^2(\tilde{v}+k)-m\mu pr]}{\mu(k+\tilde{v})^2(1+\tilde{v})}$$

Next, we substitute the values of $\tilde{v}$ and λ to obtain

$$(J-I_2)^{-1}B(q,q) = \begin{bmatrix} 0 \\ 0 \end{bmatrix},$$

and consequently

$$B\left(q,(J-I_2)^{-1}B(q,q)\right) = \begin{bmatrix} 0 \\ 0 \end{bmatrix}.$$

Finally, we evaluate $C(q,q,q)-3B\left(q,(J-I_2)^{-1}B(q,q)\right)$, then do the inner product to obtain

$$c := \frac{[p\mu(dm-4)+am(m+2)]^2[(am^3-2p\mu(m^2+4))r+a(k-1)(dm^3+2m^3+8m+16)]}{\mu^2[(am-4\mu p)r+a(k-1)(dm+4(m+1))][mr+(k-1)(dm-4)]^2}. \tag{4.6}$$

We summarize the conclusion in the follwoing result.

Theorem 4.3. *Consider Model (2.1). At $v=\tilde{v}$, if $\frac{2\mu p}{am} < \frac{k+\tilde{v}}{1+\tilde{v}} < 4\frac{\mu p}{am}$, then the coexistence equilibrium $(\bar{x}_2,\bar{y}_2)$ goes through a period-doubling bifurcation. Furthermore, the newly born 2-cycle is locally asymptotically stable when $c>0$ and unstable when $c<0$.*

We close this section by the following illustrative example.

Example 4.4. Consider the model in System (1.3), and fix

$$d=\frac{1}{10},\ p=1,\ k=5,\ \mu=\frac{7}{10},\ m=\frac{3}{10}, a=\frac{7}{5}.$$

In this case, we obtain

$$x^* = \frac{1}{14}(10r-1-v), \bar{x}_2 = \frac{1}{7}(15+3v), \quad \text{and} \quad \bar{y}_2 = \frac{(5+v)(10r-7v-31)}{10(1+v)}.$$

To have $x^* > 0$ and $\bar{x}_2 < x^*$, we need $r > \frac{31}{10}$ and $v < \frac{1}{7}(10r - 31)$. Next, we obtain $\tilde{v} = \frac{1}{259}(293 - 30r)$. Up to this end, we need $\frac{31}{10} < r < \frac{293}{30}$. At $v = \tilde{v}$, the coexistence equilibrium $(\bar{x}_2, \bar{y}_2)$ will have

$$\lambda_1 = -1 \quad \text{and} \quad \lambda = \frac{2(293 - 30r)}{5(92 - 5r)}.$$

The expression of c in Eq. (4.6) becomes

$$c = \frac{67081(20315r - 369134)}{400(85r - 1046)(15r - 794)^2},$$

which is positive on the considered values of r.

5. **Numerical simulations.** In this section, we perform numerical simulations and present bifurcation diagrams, maximum Lyapunov exponents and bi-parameter diagrams to illustrate the dynamical behaviors of the system (1.3). To investigate the impact of vigilance parameter (v) on the dynamics of the system, we set the initial value as $(0.1, 0.2)$ and run each simulation for 50000 time steps. In a dynamical system, Lyapunov exponent is a number that characterizes the rate of separation of infinitesimally nearby trajectories. We characterize chaos by the condition that the average distance between two infinitesimally close orbits magnifies exponentially with time. It is worthy to mention that in a discrete-time system, if the largest Lyapunov exponent (LLE) is positive, then the system shows chaotic oscillations, and if the LLE is negative then the system exhibits periodic or stable dynamics. It is also to be noted that in an n-dimensional system, there are n Lyapunov exponents. In the two-dimensional system (1.3), we have two Lyapunov exponents, say λ_1 and λ_2. These two Lyapunov exponents are defined as

$$\lambda_i = \lim_{K\to\infty} \frac{1}{K} \ln |\Lambda_i|, \; i = 1, 2,$$

$\Lambda_{1,2}$ being the eigenvalues of the 2×2 matrix $\Lambda = \prod_{l=1}^{K} J_l$.

Here, J_l is the Jacobian of the system (1.3) at the l-th iteration and defined by

$$J_l = \begin{pmatrix} \left(1 - \frac{ax_l}{1+v}\right) \exp\left[\frac{r}{1+v} - d - \frac{ax_l}{1+v} - \frac{py_l}{k+v}\right] & \frac{-px_l}{k+v} \exp\left[\frac{r}{1+v} - d - \frac{ax_l}{1+v} - \frac{py_l}{k+v}\right] \\ \frac{\mu py_l}{k+v} \exp\left[\frac{\mu px_l}{k+v} - m\right] & \exp\left[\frac{\mu px_l}{k+v} - m\right] \end{pmatrix}.$$

Depending on the largest (maximal) Lyapunov exponent (say λ_1), three types of topologically non-equivalent dynamical behaviors can arise. In the context of a discrete-time dynamical system, different topologically non-equivalent behaviors are given below:

(i) $\lambda_1 < 0$: fixed point/periodic attractor,
(ii) $\lambda_1 = 0$: quasi-periodic attractor,
(iii) $\lambda_1 > 0$: chaotic oscillations.

It is to be noted that at the bifurcation point the Lyapunov exponent λ_1 is also zero, but non-zero in the neighborhood of the bifurcation point [17]. Here, the Lyapunov exponents are calculated by using the above-mentioned algorithm.

5.1. **Neimark-Sacker bifurcation and chaos control.** Here, we fix the parameters as in Example 4.2, namely

$$r = 3,\ d = 0.1,\ a = 0.2,\ p = 1,\ k = 5,\ \mu = 0.7,\ m = 0.3. \tag{5.1}$$

First, we observe that in the absence of vigilance (i.e. $v = 0$), the system (1.3) shows chaotic dynamics. To visualize the impact of the vigilance parameter, we draw the bifurcation diagram and calculate the maximum Lyapunov exponent of the system with respect to the vigilance parameter v. We observe that the system becomes stable from chaotic oscillations via Neimark-Sacker bifurcation with an increase of the strength of vigilance parameter v (Fig. 4). It is observed that $D = 1$, $T = 1.8075$ and two eigenvalues of the Jacobian matrix at the interior fixed point $(3.0909, 4.6268)$ are $\lambda_{1,2} = 0.9038 \pm 0.4280\ i$ when $v = 2.212$. Therefore, the Neimark-Sacker bifurcation occurs at the point $v = 2.212$, where the other parameters are fixed at (5.1). Figure 5 shows the region of survival and extinction of the populations in $v - r$ bi-parameter space. We notice that with an increase of the value of v, populations extinct from the system. We also explore the role of vigilance on the densities of the prey and predator populations in $v-r$ bi-parameter space, where the fixed point of the system is stable. For this, we divide the $v - r$ plane ($(v, r) \in [0, 7.5] \times [0, 1.5]$) into a mesh of 800×800 different combinations of (v, r) and draw the diagram by continuously changing the color according to the values of prey and predator densities (Fig. 6). We observe that the density of the predator is high when there is no vigilance from the prey. For moderate vigilance, the density of prey is high. However, high vigilance is detrimental for both prey and predator, and the populations extinct from the system.

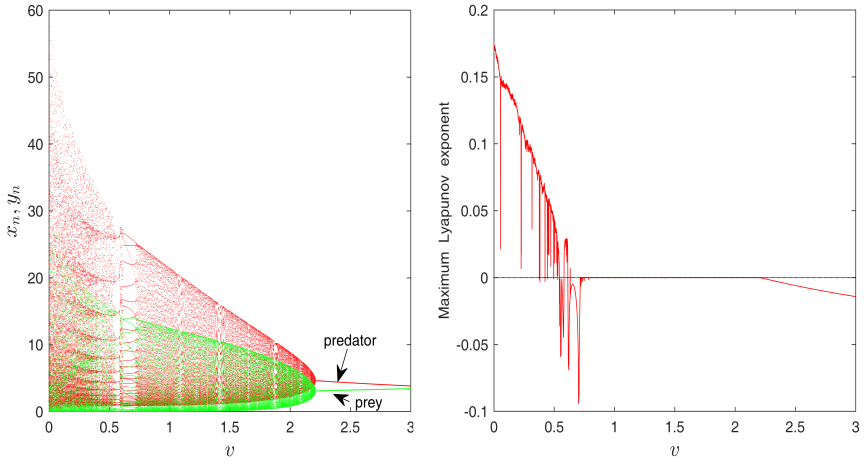

FIGURE 4. The figure shows a bifurcation diagram (left) and maximum Lyapunov exponent (right) of the system (1.3) with respect to the vigilance parameter v, where other parameters are same as equation (5.1).

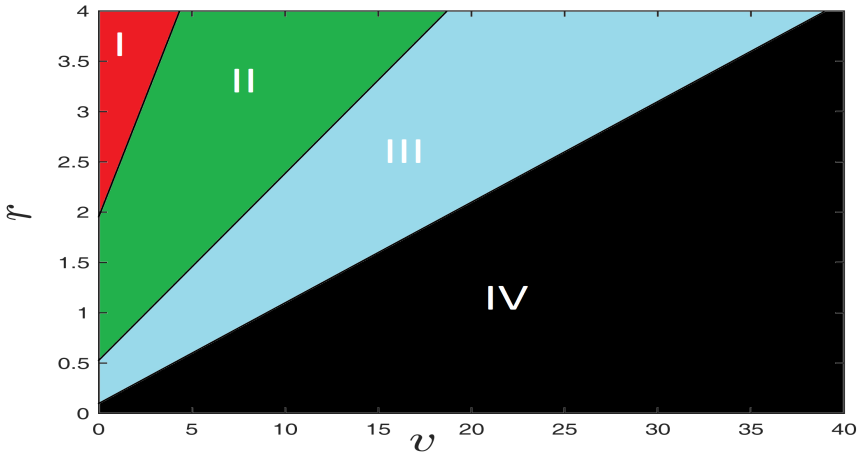

FIGURE 5. The figure shows the region of survival of the populations in $v - r$ bi-parameter space. In region I, populations show chaotic and quasiperiodic oscillations. In region II, both prey and predator show stable coexistence. In region III, the prey population shows stable behavior, but predator populations extinct from the system. In region IV, both prey and predator extinct from the system.

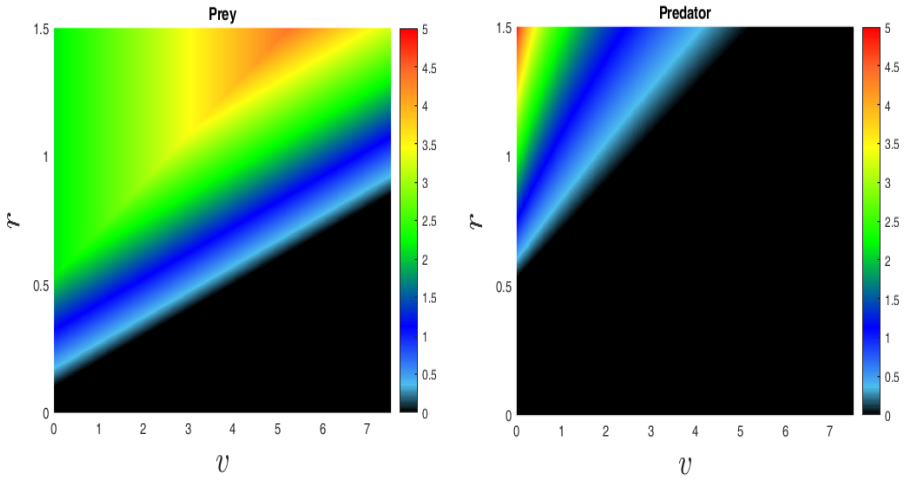

FIGURE 6. The figure shows variation of the densities of prey and predator populations in $v - r$ bi-parameter space.

Coexisting attractors: The obtained curve in the Neimark-Sacker bifurcation is topologically equivalent to a circle, and the dynamics on the circle can be interesting from a theoretical point of view. It is worth mentioning here that when we fix the parameters d, a, p, k, μ and m as in Eqs. (5.1), numerical simulations show the coexistence of different types of topologically non-equivalent attractors [18, 17]. For

$r = 2.525$ and $v = 0.046$, the system exhibits period-12 and period-13 coexisting attractors, whereas for $r = 2.659$ and $v = 0.168$, period-13 and period-14 coexisting attractors are found. Fig. 7 shows phase portraits and basins of attractions of the above-listed attractors. The period-13 attractor is highlighted by black color, and the attractors of period-12 and period-14 are in green and red colors, respectively.

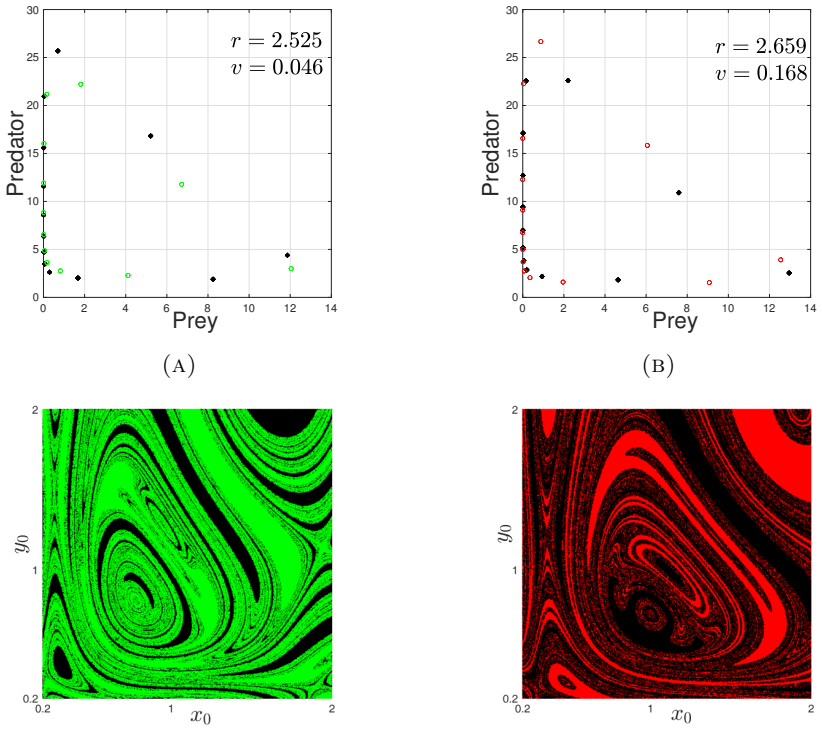

FIGURE 7. (A) Phase portrait of the system showing period-12 and period-13 attractors with initial conditions $(0.5, 0.2)$, and $(0.1, 0.2)$, (B) phase portrait of the system showing period-13 and period-14 attractors with initial conditions $(0.1, 0.2)$, and $(0.7, 0.2)$, (C) basins of attraction for the coexisting period-12 and period-13 attractors, (D) basins of attraction for the coexisting period-13 and period-14 attractors.

5.2. **Flip bifurcation and chaos control.** Here, we fix the parameters as in Example 4.4, namely

$$r = 4,\ d = 0.1,\ a = 1.4,\ p = 1,\ k = 5,\ \mu = 0.7,\ m = 0.3. \tag{5.2}$$

For the above set of parameters (5.2), we again draw the bifurcation diagram and calculate the maximum Lyapunov exponent of the system (1.3). We observe that an increase of the level of v, the system becomes stable from chaotic oscillations via period-halving bifurcation (see, Fig. 8). At $v = \tilde{v} \approx 0.668$, the equilibrium point $(\bar{x}_2, \bar{y}_2) \approx (2.4291,\ 1.4693)$ undergoes flip-bifurcation. Figure 9 shows the existence

of the populations in $v - r$ bi-parameter space and it is observed that populations go to extinction for higher values of v.

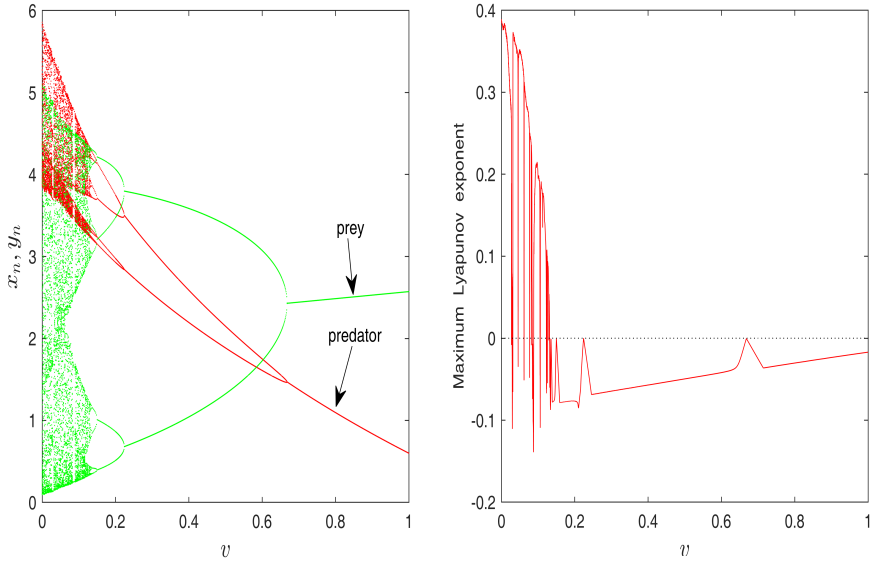

FIGURE 8. This figure shows bifurcation diagram (left) and maximum Lyapunov exponent (right) of the system (1.3) with respect to the vigilance parameter v, where other parameters are same as equation (5.2).

6. **Conclusion.** The complexity of behavioral interactions plays an important role in the dynamics and structuring of predator-prey systems. The prey population shows different types of trade-offs in behavior to reduce predation risk. In the present paper, we considered a discrete-time predator-prey model, where vigilance of prey acts as a trade-off between the safety and growth rate of the prey. We analytically and numerically investigated the stability and bifurcation behaviors of the model. We observed that vigilance drives the system towards stability from chaotic oscillations. We also noticed that the density of the predator population continuously decreased with an increase in prey vigilance due to the unavailability of food. On the other hand, with an increase of the prey vigilance, initially, the density of the prey population increased, but high vigilance had a detrimental role for the prey population as the growth rate declined significantly. We also observed the coexistence of multiple attractors in the system and drawn their basins of attractions. Therefore, depending on the initial population densities, the populations converge to different periodic cycles. So, the balance between safety and food plays an important role in the dynamics of the populations.

Finally, it is worth mentioning that this paper left several mathematical questions unanswered. Proposition 3.3 showed that the predator-free equilibrium $(x^*, 0)$ is globally asymptotically stable if $0 < \bar{x}_2 \geq x^*$ and $v \geq \frac{r}{d+1} - 1$. We believe that the conditions here are sufficient rather than necessary. In particular, we believe

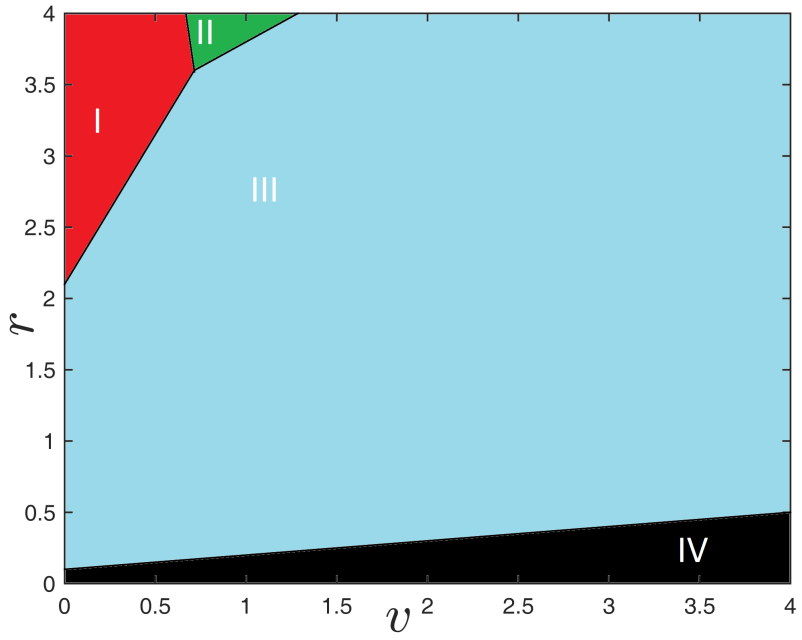

FIGURE 9. The figure shows the region of survival of the populations in $v-r$ bi-parameter space. The meanings of the regions are the same as in figure 4.

that the local stability of $(x^*, 0)$ implies its global stability. We have also utilized the notion of dissipative systems from Theorem 3.4 to prove the existence of a global attractor. The global attractor here is a set that contains the coexistence equilibrium $(\bar{x}_2, \bar{y}_2)$. However, we believe the local stability of $(\bar{x}_2, \bar{y}_2)$ implies its global stability. In particular, we believe that if $\bar{x}_2 < x^*$, $\alpha < v\beta$ and $(\beta + a - \gamma)v < \gamma + \alpha - ak$ then the coexistence equilibrium $(\bar{x}_2, \bar{y}_2)$ is globally asymptotically stable with respect to the interior of the positive quadrant.

Acknowledgments. The authors are thankful to the anonymous reviewers and the editor for their valuable comments and suggestions, which helped us in improving the quality of the manuscript. The first author was supported by an AUS grant number FRG19-S-S141, and the open access fee was covered by the Open Access Program from the American University of Sharjah. This paper represents the opinions of the authors and does not mean to represent the position or opinions of the American University of Sharjah.

REFERENCES

[1] A. S. Ackleh, M. I. Hossain, A. Veprauskas and A. Zhang, Persistence and stability analysis of discrete-time predator–prey models: A study of population and evolutionary dynamics, *J. Difference Equ. Appl.*, **25** (2019), 1568–1603.

[2] Z. AlSharawi, S. Pal, N. Pal and J. Chattopadhyay, A discrete-time model with non-monotonic functional response and strong Allee effect in prey, *J. Difference Equ. Appl.*, **26** (2020), 404–431.

[3] J. S. Brown, J. W. Laundré and M. Gurung, The ecology of fear: Optimal foraging, game theory, and trophic interactions, *Journal of Mammalogy*, **80** (1999), 385–399.
[4] S. Creel, P. Schuette and D. Christianson, Effects of predation risk on group size, vigilance, and foraging behavior in an African ungulate community, *Behavioral Ecology*, **25** (2014), 773–784.
[5] J. K. Hale, Dissipation and attractors, In *International Conference on Differential Equations,(Berlin, 1999)*, World Sci. Publ., River Edge, NJ, **1, 2** (2000), 622–637.
[6] J. K. Hale, *Asymptotic Behavior of Dissipative Systems*, volume 25 of Mathematical Surveys and Monographs, American Mathematical Society, Providence, RI, 1988.
[7] J. Hofbauer and J. W-H So, Uniform persistence and repellors for maps, *Proc. Amer. Math. Soc.*, **107** (1989), 1137–1142.
[8] J. Huang, S. Liu, S. Ruan and D. Xiao, Bifurcations in a discrete predator–prey model with nonmonotonic functional response, *J. Math. Anal. Appl.*, **464** (2018), 201–230.
[9] T. Kimbrell, R. D. Holt and P. Lundberg, The influence of vigilance on intraguild predation, *J. Theoret. Biol.*, **249** (2007), 218–234.
[10] Y. A. Kuznetsov, *Elements of Applied Bifurcation Theory*, 3^{rd} edition, Applied Mathematical Sciences, 112. Springer-Verlag, New York, 2004.
[11] S. L. Lima and L. M. Dill, Behavioral decisions made under the risk of predation: A review and prospectus, *Canadian Journal of Zoology*, **68** (1990), 619–640.
[12] M. A. Malone, A. H. Halloway and J. S. Brown, The ecology of fear and inverted biomass pyramids, *Oikos*, **129** (2020), 787–798.
[13] R. M. May, Biological populations with nonoverlapping generations: Stable points, stable cycles, and chaos, *Science*, **186** (1974), 645–647.
[14] J. D. Murray, *Mathematical Biology: I. An Introduction*, 3^{rd} edition, Interdisciplinary Applied Mathematics, 17. Springer-Verlag, New York, 2002.
[15] S. Pal, N. Pal, S. Samanta and J. Chattopadhyay, Effect of hunting cooperation and fear in a predator–prey model, *Ecological Complexity*, **39** (2019), 100770.
[16] P. Panday, N. Pal, S. Samanta and J. Chattopadhyay, Stability and bifurcation analysis of a three-species food chain model with fear, *Internat. J. Bifur. Chaos Appl. Sci. Engrg.*, **28** (2018), 1850009, 20 pp.
[17] N. C. Pati, S. Garai, M. Hossain, G. C. Layek and N. Pal, Fear induced multistability in a predator-prey model, *Internat. J. Bifur. Chaos Appl. Sci. Engrg.*, **31** (2021), 2150150, 21 pp.
[18] N. C. Pati, G. C. Layek and N. Pal, Bifurcations and organized structures in a predator-prey model with hunting cooperation, *Chaos Solitons Fractals*, **140** (2020), 110184, 11 pp.
[19] W. E. Ricker, Stock and recruitment, *Journal of the Fisheries Board of Canada*, **11** (1954), 559–623.
[20] J. P. Suraci, M. Clinchy, L. M. Dill, D. Roberts and L. Y. Zanette, Fear of large carnivores causes a trophic cascade, *Nature Communications*, **7** (2016), 10698.
[21] R. Underwood, Vigilance behaviour in grazing African antelopes, *Behaviour*, **79** (1982), 81–107.
[22] X. Wang, L. Zanette and X. Zou, Modelling the fear effect in predator–prey interactions, *J. Math. Biol.*, **73** (2016), 1179–1204.
[23] L. Y. Zanette, A. F. White, M. C. Allen and M. Clinchy, Perceived predation risk reduces the number of offspring songbirds produce per year, *Science*, **334** (2011), 1398–1401.
[24] X. Zhao, *Dynamical Systems in Population Biology*, 2^{nd} edition, CMS Books in Mathematics/Ouvrages de Mathématiques de la SMC. Springer, Cham, 2017.

Received April 2021; revised September 2021; early access February 2022.

E-mail address: zsharawi@aus.edu
E-mail address: nikhil.pal@visva-bharati.ac.in
E-mail address: joydev@isical.ac.in